

Moving forward: A review of continuous kinetics and kinematics during wheelchair and handcycling propulsion

Kellie M. Halloran^a, Michael Focht^a, Alexander Teague^b, Joseph Peters^c, Ian Rice^c, Mariana E. Kersh^{a,b,d,*}

^a*Department of Mechanical Science and Engineering, University of Illinois Urbana-Champaign*

^b*Carle Illinois College of Medicine, University of Illinois Urbana-Champaign*

^c*Department of Kinesiology, University of Illinois Urbana-Champaign*

^d*Beckman Institute for Advanced Science and Technology, University of Illinois Urbana-Champaign*

Abstract

Wheelchair users (WCUs) face high rates of upper body overuse injuries, especially in the shoulder. As exercise is recommended to reduce the high rates of cardiovascular disease among WCUs, it is becoming increasingly important to understand the mechanisms behind shoulder soft-tissue injury in WCUs to help prevent future injuries. Understanding the kinetics and kinematics during upper-limb propulsion in wheelchair users is the first step toward evaluating soft-tissue injury risk during both everyday and athletic propulsion modes. This paper examines continuous kinetic and kinematic data available in the literature for four common propulsion modes. Two everyday modes (everyday wheelchair use and attach-unit handcycling) are examined, as well as two athletic modes (wheelchair racing and recumbent handcycling). These athletic modes are important to characterize, especially considering the higher contact forces, speed, and power outputs often experienced during these athletic propulsion modes that could be putting users at increased risk of injury. Understanding the underlying kinetics and kinematics during various propulsion modes can lend insight into shoulder loading, and therefore injury risk, during these activities and inform future exercise guidelines and programs for WCUs.

Keywords: exercise, physical activity, racing, cardiovascular disease, propulsion, shoulder, handrim, handcrank

1. Introduction

In the United States, an estimated 5.5 million people rely on wheelchairs for their primary means of locomotion⁽¹⁾ due to a variety of conditions including congenital defects, spinal cord injuries, movement disorders, and stroke^(1,2). Though many may associate the elderly as the most prevalent demographic among wheelchair users (WCUs), almost half of WCUs are under the age of 65^(1,3). As mobility impairments are often permanent, WCUs depend on their wheelchairs and upper extremities for ambulation. Unfortunately, the transition to wheelchair use and increase in loading cycles as a result of wheelchair-related activities may place the upper extremity at increased risk for injury^(4,5,6,7,8).

For example, 40-75% of WCUs report upper extremity injury and pain, often at the shoulder^(9,10,11,12), which is attributed to overuse from wheelchair propulsion and transfers⁽¹³⁾. This increased loading of the upper arm has been suggested to result in degenerative morphological changes in the shoulder soft tissue⁽¹⁴⁾, rotator cuff impingement⁽¹⁵⁾, and rotator cuff tendinopathy^(6,7,16). Even more concerning is that up to 98% of WCUs demonstrate radiographic evidence of shoulder injury including asymptomatic users^(16,6). In the general population, nearly 60% of all rotator cuff injuries are asymptomatic⁽¹⁷⁾. The biomechanical challenges facing WCUs are compounded by the need for increased exercise to help mitigate cardiovascular disease (CVD).

It is well established that physical inactivity in WCUs increases the rates of obesity, diabetes, hypertension, and dyslipidemia^(18,19), which are all major risk factors for CVD. In fact, people with spinal cord injuries have an over 50% higher risk of CVD than the general population⁽²⁰⁾. Despite clear evidence supporting the benefits of exercise, engagement in

*Corresponding author: mkersh@illinois.edu (Mariana E. Kersh)

exercise is low in WCUs due to socioecological, institutional, and interpersonal challenges^(21,22). Adaptive sports are both physically and psychologically beneficial for people with spinal cord injuries⁽²³⁾, have grown in popularity among WCU's in recent years⁽²⁴⁾, and thus present an opportunity to improve cardiovascular function. From a biomechanical perspective, as upper limb health is of paramount importance to WCU populations, it is essential that an exercise intervention does not contribute to or worsen upper limb pain.

Our understanding of shoulder function can be informed by computational methods that combine in vivo biomechanical data (kinematics, kinetics) with musculoskeletal models of the body. One modeling technique involves the use of rigid-body systems based on subject-specific anthropometrics to simulate different tasks using collected kinematic and kinetic data. The outputs of rigid-body dynamics models include joint accelerations, joint torques, muscle forces, and joint contact forces^(25,26,27,28). When combined with computational models at the tissue level, it is possible to obtain estimates of strains. Such models have been used to evaluate rotator cuff tears^(29,30), and have the potential to determine whether a given exercise type may or may not place the shoulder at risk of injury.

Critical to computational analyses of shoulder biomechanics during wheelchair usage is the underlying kinematic and kinetic data. As such, the purpose of this review is to summarize existing literature that reports continuous kinetic and kinematic data during common locomotion modes used by WCUs. Within this review, we first give an introduction to wheelchair biomechanics and commonly used terms (Section 2) and describe our methodology for selection of papers and data reduction (Section 3). Next, we summarized kinematic and kinetic data for two types of propulsion: handrim (Section 4) and crank (Section 5). Within each propulsion type we compared everyday usage to athletic forms.

2. Activities

There are two common types of propulsion modes used by WCU's: handrim propulsion and crank propulsion. Everyday wheelchair use is an example of handrim propulsion, where the user pushes a rim on the wheel to move forward. In contrast, crank propulsion (such as during handcycling), uses a gear system

to convert rotational handcrank motion into forward wheel motion. Within handrim and crank propulsion are modes for athletic propulsion: wheelchair racing and recumbent handcycling, respectively.

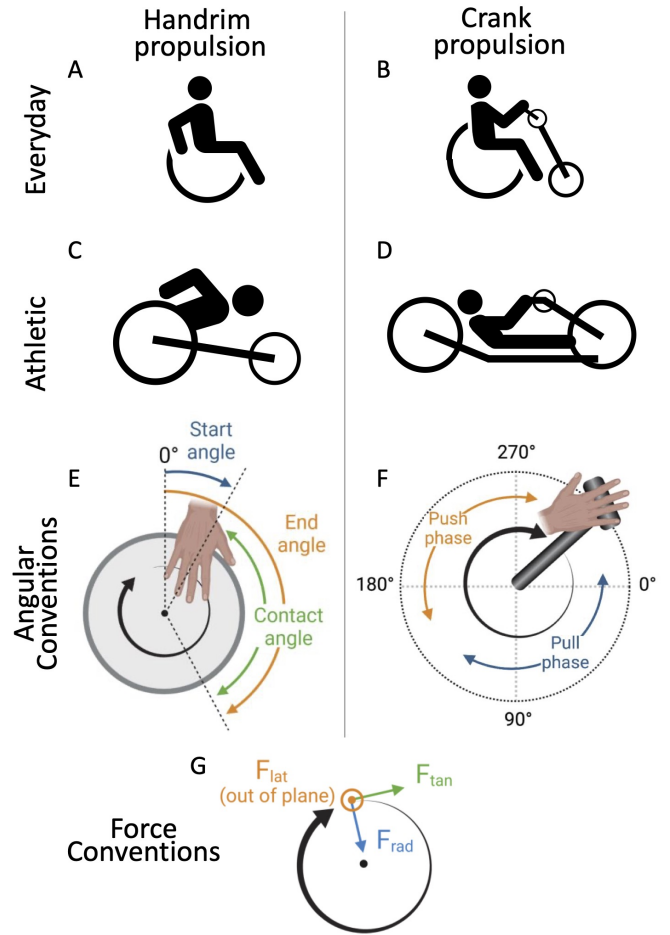


Figure 1: Propulsion modes: A) everyday wheelchair propulsion, B) attach-unit handcycling, C) racing wheelchair propulsion, D) recumbent handcycling. Angle conventions (right-hand side) and propulsion phases for E) handrim propulsion and F) crank propulsion. G) Force conventions used.

2.1. Handrim Propulsion

Everyday propulsion features an upright wheelchair and is the typical mode used by most WCU's for locomotion (Fig 1A). These wheelchairs typically feature two large wheels, one on either side of the user, that are perpendicular to the ground along with smaller front wheels for balance. A propulsion cycle involves grabbing the handrim and pushing followed by a hand recovery path where no handrim contact occurs⁽³¹⁾. While some exercise can be done in an upright wheelchair, WCUs switch

from an everyday wheelchair to a racing wheelchairs to achieve faster speeds.

Racing wheelchairs also have two large wheels, but they are placed at a camber angle for added stability and improved speed and performance compared to the everyday wheelchair⁽³²⁾. Rather than two smaller wheels, racing wheelchairs have one medium-sized wheel in the front which improves the chair's aerodynamics and enables higher speeds (Figure 1C). Racing wheelchairs are propelled in a crouched kneeling position, with the user leaning forward compared to the upright sitting position of everyday wheelchair propulsion. Instead of grabbing the handrim, propulsion occurs with an individual "punching" the handrim, usually with a glove or hard hand-held implement⁽³²⁾.

In both handrim propulsion modes, the kinematics are split into two phases: the push phase, where the hand is in contact with the wheel rim, and the recovery phase, where the hand is in the air. The length of the push phase corresponds to the magnitude of the contact angle defined as the end angle minus the start angle (Fig 1E).

2.2. Crank Propulsion

Crank propulsion is an alternative mode of locomotion to wheelchair propulsion and is typically done on a handcycle. The gears on a handcycle offer a greater mechanical advantage than handrim propulsion and are suggested to create a more efficient mode of transportation⁽³³⁾. Attach-unit handcycles use a third wheel and crank system attached to an everyday handrim wheelchair (Fig 1B). Sport handcycles (Fig 1D) are usually recumbent, featuring a reclined backrest that places the body closer to the ground in a more aerodynamic position. Handcycle propulsion differs from handrim propulsion in that the hand is in contact with the crank at all times. One cycle of the handcycle crank is split into two phases: the pull phase and push phase (Fig 1F). During the pull phase, the user is pulling the crank toward themselves; during the push phase, the user is pushing the handle away from the body.

For the purposes of this review, we report force data using polar conventions. Tangential force, the force parallel to the wheel or crank path, is positive when in the direction of rotation. Positive radial force was defined as the force pointing towards the center of the wheel or center of handcycle rotation, and lateral force, which is the force out of the sagittal plane, was

defined as positive if it was pointing in the lateral direction (away from the user).

3. Methods

Retrieval of papers was performed using Google Scholar and Pubmed with combinations of the following keywords: "Wheelchair", "Kinetics", "Kinematics", "Forces", "Handcycle", and "Inverse Dynamics". Forward and backward citation searches were used to find additional studies. Studies reporting kinematic and kinetic data were included if the authors reported continuous data. Studies reporting discrete (single time point) kinetic or kinematics data were excluded. Studies reporting force data in the global x,y,z coordinate system but not the tangential, radial, and lateral components were also excluded. In the 1990s, most racers shifted from an upright sitting position to a forward, crouched position⁽³¹⁾. Thus, racing wheelchair propulsion studies published before 1990 were excluded from this review.

Continuous kinematic or kinetic data from published figures were digitized using WebPlotDigitizer. At least 15 data points were digitized per plot. Data were processed in MATLAB and Microsoft Excel. For handrim propulsion, only data from the push-phase was analyzed and was normalized by length of push phase. Joint angle descriptions are adapted from International Society of Biomechanics (ISB) conventions⁽³⁴⁾ for the shoulder (Fig S1).

When multiple propulsion cycles were reported per test condition (e.g. same speed, PO, or trial), each cycle was digitized and the cycles were averaged to obtain a representative curve from the test condition. In some cases, data from multiple studies were combined using a weighted average based on the number of study participants. All figures were rendered in R.

4. Handrim Propulsion

4.1. Everyday Wheelchairs: Kinetics

With the development of the SmartWheel in the 1990's, it became feasible to record three-dimensional handrim forces during wheelchair propulsion and provide insight into loading of the upper extremity.

To our knowledge, three studies have reported continuous tangential, radial, or lateral handrim force components during everyday wheelchair use^(35,36,37). The maximum tangential forces range from 29 to 108 N (Fig 2A) and are on average greater than the range

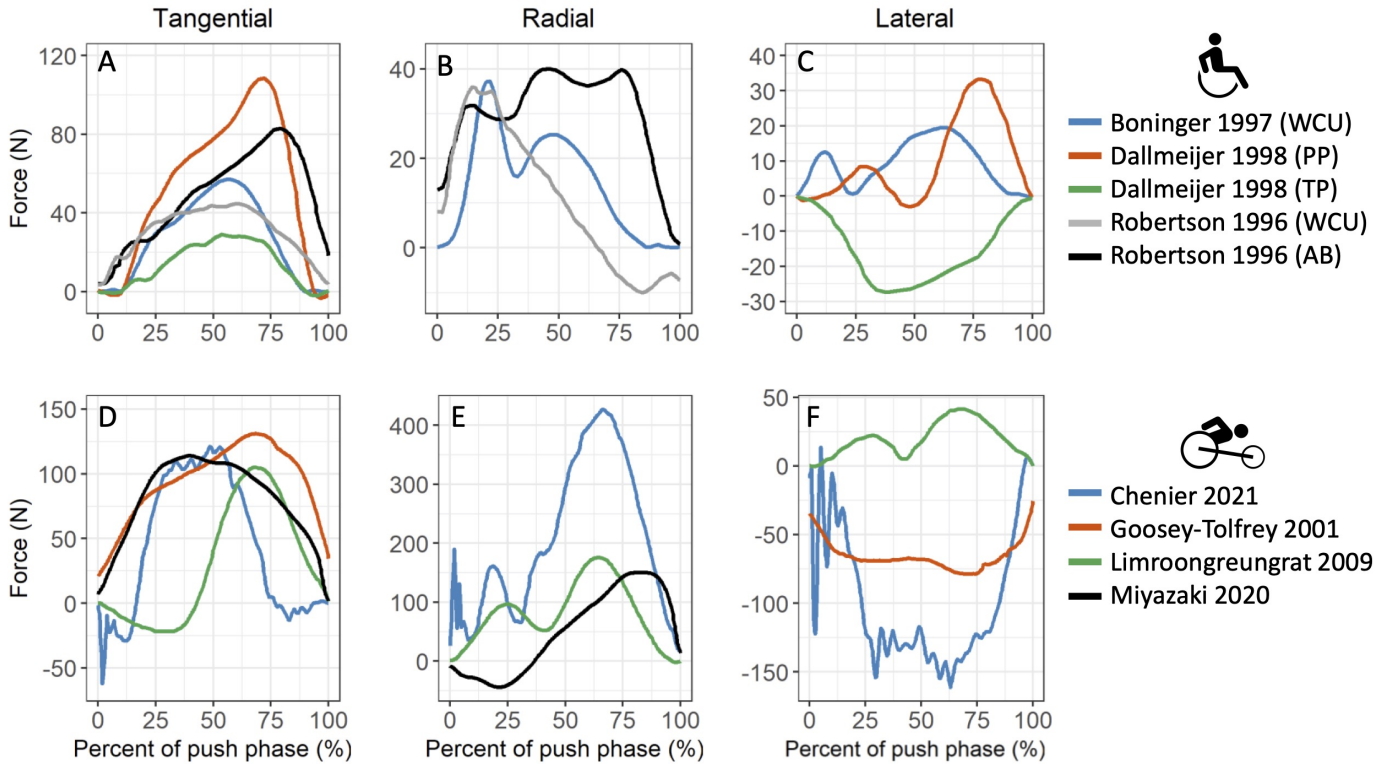


Figure 2: Applied handrim forces (N) during everyday wheelchair propulsion (top row) and racing wheelchair propulsion (bottom row) by A,D) tangential component, B,E) radial component, and C,F) lateral component. PP = paraplegic subject, TP = tetraplegic subject, AB = able-bodied subject, WCU = wheelchair user.

of maximum radial forces (36-40 N, Fig 2B) or lateral forces (19-33 N, Fig 2C). Tangential forces have a single peak in the last half of the push phase (54-79%) whereas radial and lateral forces have multiple peaks.

Radial forces tend to reach a maximum early in the push phase (14-22%). In contrast, lateral forces tend to have two peaks: an initial lower peak in the first half of the push phase (12-27%) followed by a higher peak in the second half of the push phase (63-78%).

Differences in the magnitude of the tangential forces may be due to different wheelchair setups and speeds used during testing. For example, the largest reported tangential forces occurred with subjects propelling at 60-80% of peak power outputs⁽³⁶⁾ while the other force profiles likely occurred at lower speeds (range: 1.5-2.0 m/s)^(37,35). Experienced wheelchair users tended to apply lower peak tangential forces ($p=0.0001$) and took longer to reach the peak tangential forces ($p=0.0015$) than able-bodied participants⁽³⁷⁾, though one exception is reported from Dallmeijer and colleagues⁽³⁶⁾.

Notably, the lateral force component reported from a subject with tetraplegia⁽³⁶⁾ was negative and with a single peak while others report positive double-

peaked lateral forces. Whether or not the location and severity of spinal cord injury affects the loads applied during propulsion remains to be clearly demonstrated, but these data suggest that care should be taken when interpreting wheelchair kinetics from participants of varying injury levels.

4.2. Wheelchair Racing: Kinetics

An examination of the studies that report continuous applied forces during racing wheelchair propulsion yields results with high variability in both the shape of the force curves and the location of peak forces (Fig 2D-F). In contrast to everyday wheelchair usage, the maximum forces were applied radially during racing wheelchair propulsion. As expected due to increased speeds, the average maximum applied forces during racing propulsion were larger for all magnitudes of components compared to everyday propulsion (118 vs. 64 N for tangential forces, 251 vs. 38 N for radial forces, and 94 vs 26 N for lateral forces in racing vs. everyday propulsion, respectively). Similar to everyday wheelchair propulsion, the maximum tangential forces (range: 105-131 N, Fig 2D) during racing propulsion peaks once in the middle of the

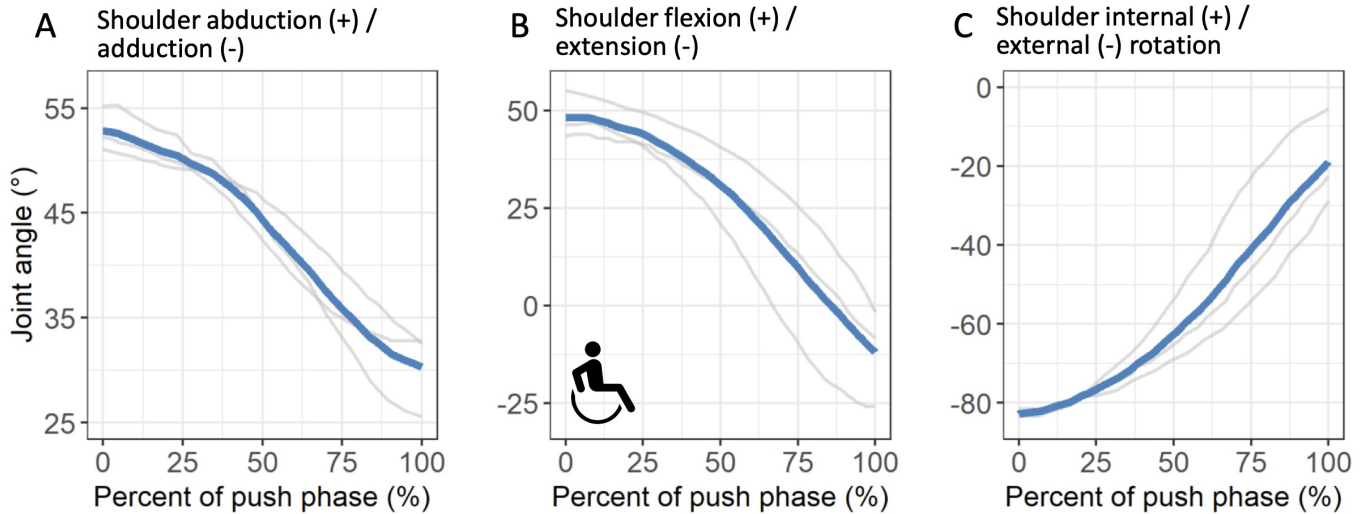


Figure 3: Joint angles ($^{\circ}$) during the push phase of everyday wheelchair propulsion, averages in blue. ^(38,39)

push phase (40-69%) compared to the latter part of the push phase during wheelchair propulsion.

245 Also similar to everyday, radial forces during racing peaked multiple times with maximum forces ranging from 150-428 N, but all force profiles peaked in the second half of the push phase (64-82%) compared to earlier peaks at the beginning of the push phase for everyday propulsion (Fig 2E). Chenier et al. reported maximum radial forces of 427 N, which they attribute to the design of the force measurement system and the fact that their participant was propelling at maximum speed⁽⁴⁰⁾. In contrast to everyday propulsion, 250 two of the three racing studies reported negative lateral forces but with inconsistent force profiles. The positive lateral forces reported by Limroongreungrat et al. were attributed to differences in wheelchair design and propulsion speed⁽⁴¹⁾.

260 4.3. Everyday Wheelchairs: Kinematics

Kinematic profiles of the shoulder within the two studies reporting shoulder angles using the ISB conventions were consistent. Wheelchair propulsion begins with the shoulder abducted to 53° , flexed to 48° , and externally rotated by -83° (Fig 3A-C, respectively). During the push phase, the shoulder adducts to 30° , extends to -12° , and internally rotates to -19° .

265 Boninger et al.⁽⁴²⁾ and Koontz et al.⁽⁴³⁾ also reported continuous shoulder angles, but these studies were done prior to ISB shoulder angle conventions and used projections of the humerus in the anatomical planes. As a result, these shoulder angles were not included in our analysis but are worth noting as sources of continuous kinematic data.

4.4. Wheelchair Racing: Kinematics

275

Few studies report continuous joint angle data during racing propulsion using the current (post-1990's) racing wheelchair design. To our knowledge, two studies have reported continuous joint angles, but only reported elbow flexion^(44,45). Moss et al.⁽⁴⁶⁾, who reported start and end angles of a sprint start during wheelchair racing, was also excluded from analysis due to the altered technique associated with static propulsion mechanics.

280

285 There are however reports of the start and end angles during propulsion (Fig 4). These contact angles are important to quantify because the length of the push phase affects the length of time that the shoulder experiences applied forces⁽⁴⁷⁾. In racing propulsion, the mean start angle is 27.8° and the mean end release angle is 197° , on average (Fig 4). The resulting contact angle of 169° indicates that the hand is in contact with the handrim and transferring forces for almost half of the propulsion cycle. In everyday propulsion, the average push angle is 83° .

285

290

295

Start angles and end angles vary depending on the handrim propulsion mode, with everyday propulsion having a smaller and more precise push phase compared to racing propulsion. The increased variability in the push phase for racing propulsion could be attributed to racing technique (recovery path location, having a tightly closed fist or using the thumb to apply force, etc.) based on personal preference and race length^(48,49).

300

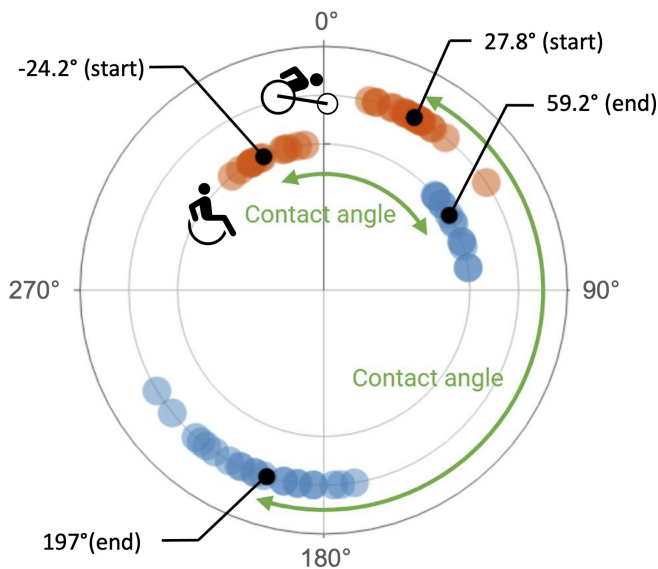


Figure 4: Handrim contact and release angles for racing^(50,49,48,51,52,53,46,44,47) and everyday^(36,43,54,55,56,57) propulsion. Mean angles for each activity are shown in black.

4.5. Implications of handrim wheelchair vs racing propulsion

In general, the maximum applied force components during racing wheelchair propulsion are 1.2-10.7 times larger than those recorded during everyday wheelchair propulsion. This increase is likely due to the high speeds and intensities associated with racing. Whether these increased force values may be placing the shoulder at increased risk for injury remains to be clearly demonstrated, though Mercer et al. have shown that increased lateral forces are associated with pain and injury⁽⁵⁸⁾. The wide range of force values and profiles across studies points to the need to more fully examine the applied forces of racing propulsion including larger sample sizes with a more consistent method of measuring applied forces.

The lack of shoulder kinematic data during racing prevents a direct comparison to everyday wheelchair usage. However, the start and end angles can also lend insight into changes in propulsion styles. While the longer (2 times the contact angle) push phase in racing compared to everyday propulsion may indicate more time for force transfer, and therefore less impact on the shoulder, racing propulsion also results in increased forces. It is still unclear how the combination of increased forces and larger contact angle during racing propulsion affects shoulder joint loading, and therefore tissue strain and injury risk.

The force transfer during wheelchair propulsion is

also dependent on propulsion kinematics: increased shoulder elevation, and shoulder rotation are correlated with increased shoulder joint reaction forces during racing propulsion, which is indicative of higher shoulder injury risk⁽⁴⁷⁾. Thus, it is important to more carefully quantify how the upper arms are moving during wheelchair racing propulsion to optimize force transfer from an injury prevention standpoint.

5. Crank Propulsion

With the introduction of a crank for propulsion, applied forces and movement shift from the period associated with the push angle of propulsion to continuous biomechanical data throughout a complete propulsion cycle. One should note that the origin for the angular phases during crank propulsion is different (anterior) than the origin used for handrim propulsion (proximal).

5.1. Attach-unit Handcycling: Kinetics

Two studies have reported continuous forces during attach-unit handcycling, with only one study⁽⁵⁹⁾ reporting all three force components. The tangential force profiles have similar shapes and primarily differ in the magnitude of the forces (Fig 5). The largest peak tangential force recorded was 45 Newtons and occurred between 64° and 91° of the cycle (Fig 5). The transition from push to pull phase is indicated by the local minimums of tangential forces which occurred between 276° and 310°. As rolling resistance increased, shown via increases in Watts, tangential forces also increased to maintain speed⁽⁶⁰⁾. Able-bodied subjects cycling at 1.94 m/s had lower tangential forces⁽⁶⁰⁾ than those reported in a subject with paraplegia cycling at 35W⁽⁵⁹⁾.

5.2. Recumbent Handcycling: Kinetics

To our knowledge, only one study has reported direct measurements of continuous applied forces during recumbent handcycling (Fig 6A)⁽⁶⁶⁾. Ahlers and Jakobsen report a maximum tangential force of 127 N at 107° in the propulsion cycle, with a pronounced push-pull and pull-push transition at 2° and 199°, respectively. Several studies have investigated the effect of changing either the handcycle configuration (i.e. crank length, backrest angle, crank position, etc.) or the power output during propulsion and reported continuous torque during recumbent handcycling.

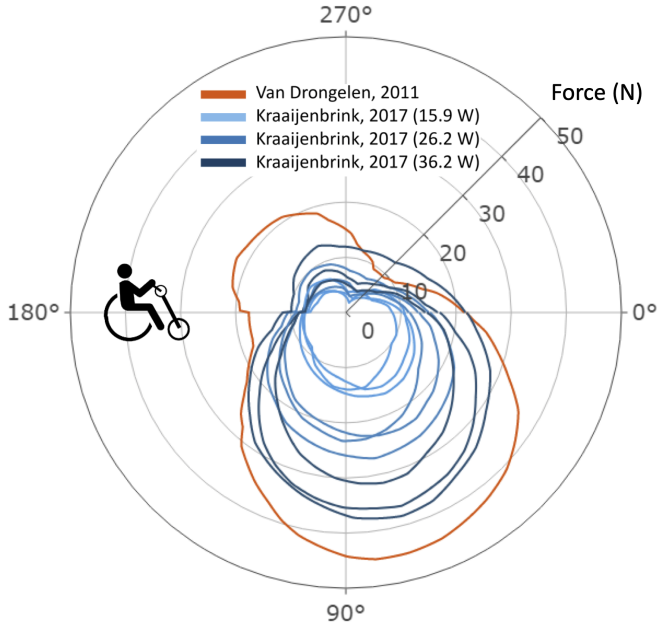


Figure 5: Tangential force (N) during attach-unit handcycling^(59,60). The three shades of blue represent three resistance levels, but at varying gear levels.

cling^(64,65,62,63). This torque data can be used to indirectly calculate F_{tan} using Equation 1:

$$F_{tan} = \tau / R \quad (1)$$

where τ is the torque at the crank and R is the crank length. Changes in crank length do not significantly change the applied torque profiles⁽⁶²⁾ (Fig 6B, blue lines). However, torques are sensitive to the crank position⁽⁶³⁾: when the crank is moved closer to the participant, the torque in the push phase increases and torque in the pull phase decreases (Fig 6B). The tangential forces during recumbent handcycling kinetics are also sensitive to changes in power output with maximum force increasing with increasing power.

The location of maximum force across studies was variable (range = 34°- 273°), and could be a result of varying levels of handcycling experience, handcycling design, participant demographics, and different methodologies in collecting force data. The location of the push-pull transition (291°-2°) and pull-push transition (132°-199°) (Fig 1F), defined as the location of minimum applied force, were more consistent across studies though studies investigating the effect of power (Fig 6C) did not report a clear transition point. Compared to attach unit handcycling, the push-pull transition occurs later in the propulsion cycle. It is worth noting that the study directly measuring F_{tan} (Fig 6A) has a force profile similar to that recorded during attach unit handcycling, with the

maximum tangential force occurring at the bottom of the propulsion cycle (Fig 5). It's possible that, with more consistent data collection methods across recumbent and attach-unit handcycling, a clearer tangential force curve would emerge.

5.3. Attach-unit Handcycling: Kinematics

We did not find any studies that reported continuous joint angles during attach-unit handcycling. Faupin and Gorce reported the maximum and minimum shoulder angles for one able-bodied participant and one participant with paraplegia during 70 rpm handcycling⁽⁷⁰⁾. They reported a 63, 19, and 11 degree range of motion for shoulder flexion, abduction, and rotation, respectively, for the able-bodied participant. The range of motion for the subject with paraplegia was greater than the able-bodied subject, with 71, 23, and 17 degree ranges of motion for shoulder flexion, abduction, and rotation, respectively.

5.4. Recumbent Handcycling: Kinematics

In contrast to attach-unit handcycling, continuous kinematic data during recumbent handcycling has been reported. Handcycling begins with the shoulder in abduction after which it continues to abduct by 31°, followed by adduction to 10°(Fig 7A). Average maximum abduction of 31° occurs at 199° in the propulsion cycle. There is a slight increase in shoulder abduction with an increase in power output: as the intensity of the exercise increased, the shoulder becomes more elevated and abducts up to 39°. Shoulder flexion exhibits two peaks during recumbent handcycling: initially the shoulder is flexed to X° and then extends to -19° followed by a return to flexion which peaks at 300° towards the end of the propulsion cycle (Fig 7B).

The variation between studies in shoulder abduction and flexion was less than the variation in shoulder internal / external rotation (Fig 7C). Studies that used acromion marker clusters⁽⁷¹⁾ to track scapular movement reported a wider variation in shoulder rotation, from -10° to 45°^(68,62). The studies that did not use an acromion cluster to track scapula kinematics reported a smaller range of shoulder rotation, from about 10° to 25°^(64,67).

5.5. Implications for attach unit vs recumbent handcycling

During sprinting, the tangential applied forces reach a maximum of 447 N, which is more than ten

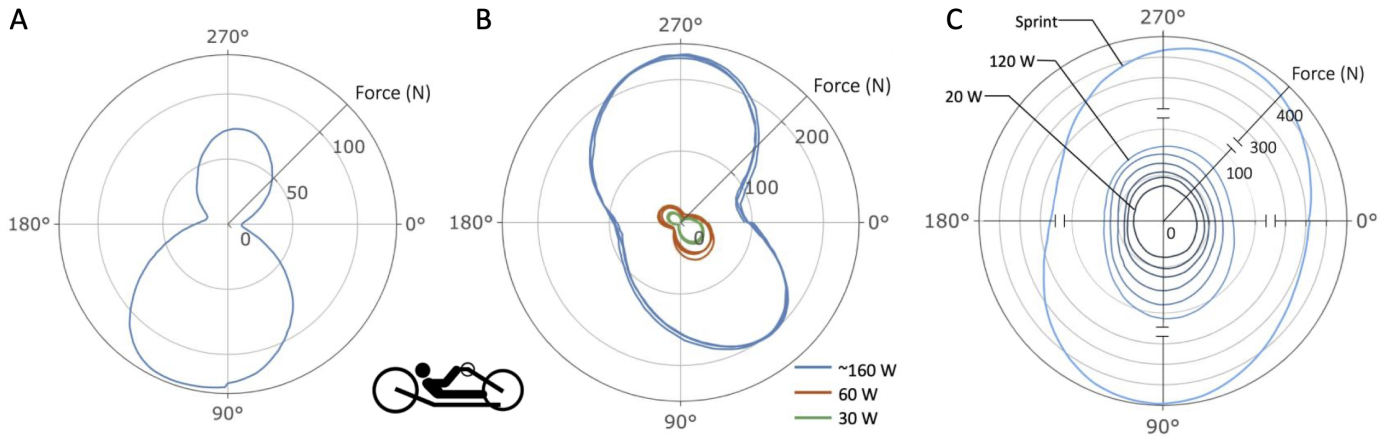


Figure 6: Tangential applied force (F_{tan}) (N) during recumbent handcycling. Studies examining A) F_{tan} measured directly using a strain gauge-instrumented handle, self-selected speed⁽⁶¹⁾, B) changes in handcycle configuration (changes in crank length shown in blue⁽⁶²⁾, and changes in crank fore-aft position, as a percentage of arm length, shown in orange and green⁽⁶³⁾) and C) changes in power (20-120W)⁽⁶⁴⁾ and sprinting⁽⁶⁵⁾.

440 times larger than the maximum tangential forces reported during attach-unit handcycling. When athletes train at increased speeds and power outputs, it is reasonable to suggest that these increased external forces will result in increased loads at the shoulder.
 445 The question remains as to which power or speed levels, and for how long, are acceptable to avoid overuse injuries common in wheelchair athletes. Additionally, only continuous F_{tan} data was available in the literature for recumbent handcycling. While F_{tan} is the majority of the total applied force during attach-unit handcycling, it's still unclear how the other components (radial and lateral) are impacted by changes in recumbent handcycle configurations and power.
 450 Force changes for all three directions are important for modeling the upper extremities and understand-
 455

ing musculoskeletal loads during any activity including recumbent handcycling⁽⁷²⁾.

Kinematics differences are also important: the elevated positions associated with increased power have been suggested as a source of increased risk for injury⁽⁷³⁾. Because of the lowered body position in recumbent handcycling, participants are propelling with their arms at more elevated positions compared to attach-unit handcycling. Other overhead sport activities (i.e., swimming, volleyball, gymnastics), which also involve elevated shoulder angles, are considered to put the shoulder at more injury-prone positions⁽⁷³⁾. This is consistent with findings by Arnet et al. who confirmed that a more inclined backrest position (more recumbent) leads to higher shoulder loads in attach-unit handcycling⁽⁷⁴⁾. While the

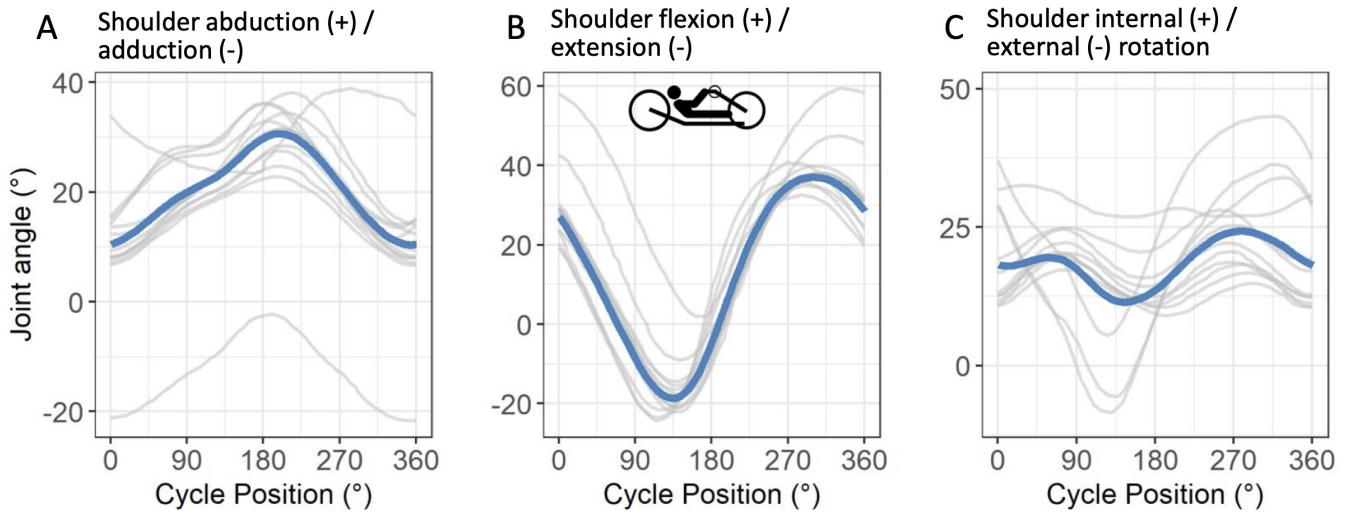


Figure 7: Recumbent handcycling joint angles ($^{\circ}$), averages in blue.^(67,62,64,65,68,69)

impact of shoulder rotation on shoulder soft tissue strain hasn't been quantified for recumbent handcycling, higher internal rotation was identified as a risk factor during weight bearing activities for shoulder pain in WCUs⁽⁷⁵⁾. Nonetheless, more data is needed to identify potential stages during crank propulsion when the load on the shoulder is highest to optimize training protocols to reduce injury risk.

While this is a promising start, a more thorough investigation of the three-dimensional shoulder loads during recumbent handcycling using models specific to WCUs could provide insight into injury risk and prevention techniques, especially at the higher speeds experiences during recumbent handcycling races and exercise.

6. Conclusion

Upper extremity injuries and CVD in WCUs represent a multi-factorial problem with an evidenced burden on individuals and society. A greater understanding of upper-limb kinetics and kinematics during propulsion can lend insight into joint loading, and therefore joint forces and injury risk, faced by WCUs during both handrim and crank propulsion. In general, the applied hand forces are larger for both athletic propulsion modes (racing wheelchair propulsion and recumbent handcycling). These increased forces could indicate increased shoulder loading during these activities. While this data is a promising start to characterizing the biomechanics of common propulsion modes in WCUs, there is still work to be done. With continuous kinetic and kinematic data, upper limb rigid-dynamics models can be created that calculate joint torques and accelerations, joint contact forces, and muscle forces, which can lend insight into shoulder injury risk. There is still a need to more completely characterize shoulder joint angles during racing wheelchair propulsion and continuous three-dimensional forces during recumbent handcycling. Once these propulsion styles are more completely characterized, we can develop predictive models for coaching, training, and physical therapy to reduce shoulder injury risk and increase the quality of life for WCUs.

515 References

- [1] Danielle M Taylor. Americans with Disabilities: 2014. *Current Population Reports*, pages 1–32, 2018.
- [2] Amol M. Karmarkar, Brad E. Dicianno, Rosemarie Cooper, Diane M. Collins, Judith T. Matthews, Alicia Koontz, Emily E. Teodorski, and Rory A. Cooper. Demographic profile of older adults using wheeled mobility devices. *Journal of Aging Research*, 2011, 2011.
- 520 [3] Emma M. Smith, Edward M. Giesbrecht, W. Ben Mortenson, and William C. Miller. Prevalence of wheelchair and scooter use among community-dwelling Canadians. *Physical Therapy*, 96(8):1135–1142, 2016.
- 525 [4] Robert S. Burnham, Laura May, Ewen Nelson, Robert Steadward, and David C. Reid. Shoulder pain in wheelchair athletes: The role of muscle imbalance. *Technical Report 2*, 1993.
- 530 [5] J. V. Subbarao, J. Klopstein, and R. Turpin. Prevalence and impact of wrist and shoulder pain in patients with spinal cord injury. *The journal of spinal cord medicine*, 18(1):9–13, 1995.
- 535 [6] Omid Jahanian, Meegan G. Van Straaten, Brianna M. Goodwin, Ryan J. Lennon, Jonathan D. Barlow, Naveen S. Murthy, and Melissa M.B. Morrow. Shoulder magnetic resonance imaging findings in manual wheelchair users with spinal cord injury. *Journal of Spinal Cord Medicine*, 0(0):1–11, 2020.
- 540 [7] Tiffany K. Gill, E. Michael Shanahan, Dale Allison, Daniel Alcorn, and Catherine L. Hill. Prevalence of abnormalities on shoulder MRI in symptomatic and asymptomatic older adults. *International Journal of Rheumatic Diseases*, 17(8):863–871, 2014.
- 545 [8] Timo Hinrichs, Veronika Lay, Ursina Arnet, Inge Eriks-Hoogland, Hans Georg Koch, Taina Rantanen, Jan D. Reinhardt, Martin W.G. Brinkhof, Olivier Dériaz, Michael Baumberger, Hans Peter Gmünder, Armin Curt, Martin Schubert, Margret Hund-Georgiadis, Kerstin Hug, Hans Georg Koch, Urs Styger, Hardy Landolt, Hannjörg Koch, Mirjam Brach, Gerold Stucki, Martin Brinkhof, and Christine Thyrian. Age-related variation in mobility independence among wheelchair users with spinal cord injury: A cross-sectional study. *Journal of Spinal Cord Medicine*, 39(2):180–189, 2016.
- 550 [9] M. Dalyan, D. D. Cardenas, and B. Gerard. Upper extremity pain after spinal cord injury. *Technical Report 3*, 1999.
- 560 [10] Marie Alm, Helena Saraste, and Cecilia Norrbrink. Shoulder pain in persons with thoracic spinal cord injury: Prevalence and characteristics. *Journal of Rehabilitation Medicine*, 40(4):277–283, 2008.
- 565 [11] Kathleen A. Curtis and Deborah A. Dillon. Survey of wheelchair athletic injuries: Common patterns and prevention. *Technical Report 3*, 1985.
- [12] Margaret A Finley, Elizabeth K Rasch, Randall E Keyser, and Mary M Rodgers. The biomechanics of wheelchair propulsion in individuals with and without upper-limb impairment. *Technical report*, 2004.
- 570 [13] D. B. Barber and M. D. Gall. Osteonecrosis: An overuse injury of the shoulder in paraplegia: Case report. *Paraplegia*, 29(6):423–426, 1991.
- [14] Steven W. Brose, Michael L. Boninger, Bradley Fullerton, Thane McCann, Jennifer L. Collinger, Bradley G. Impink, and Trevor A. Dyson-Hudson. Shoulder Ultrasound Abnormalities, Physical Examination Findings, and Pain in Manual Wheelchair Users With Spinal Cord Injury. *Archives of Physical Medicine and Rehabilitation*, 89(11):2086–2093, 2008.
- 580 [15] J. C. Bayley, T. P. Cochran, and C. B. Sledge. The weight-bearing shoulder. The impingement syndrome in paraplegics. *Journal of Bone and Joint Surgery - Series A*, 69(5):676–678, 1987.
- [16] Santosh Lal. Premature degenerative shoulder changes in spinal cord injury patients. *Spinal Cord*, 36(3):186–189, 1998.
- 585 [17] Hiroshi Minagawa, Nobuyuki Yamamoto, Hidekazu Abe, Masashi Fukuda, Nobutoshi Seki, Kazuma Kikuchi, Hiroaki Kijima, and Eiji Itoi. Prevalence of symptomatic and asymptomatic rotator cuff tears in the general population: From mass-screening in one village. *Journal of Orthopaedics*, 10(1):8–12, 2013.
- 590 [18] David R. Gater, Gary J. Farkas, Arthur S. Berg, and Camilo Castillo. Prevalence of metabolic syndrome in veterans with spinal cord injury. *Journal of Spinal Cord Medicine*, 42(1):86–93, 2019.
- 595 [19] W. Barry, J. R. St Andre, C. T. Evans, S. Sabharwal, S. Miskevics, F. M. Weaver, and B. M. Smith. Hypertension and antihypertensive treatment in veterans with spinal cord injury and disorders. *Spinal Cord*, 51(2):109–115, 2013.
- 600 [20] Sherri L. LaVela, Charlesnika T. Evans, Thomas R. Prohaska, Scott Miskevics, Shanti P. Ganesh, and Frances M. Weaver. Males aging with a spinal cord injury: prevalence of cardiovascular and metabolic conditions. *Archives of Physical Medicine and Rehabilitation*, 93(1):90–95, 2012.
- 605 [21] Matthew Kehn and Thilo Kroll. Staying physically active after spinal cord injury: A qualitative exploration of barriers and facilitators to exercise participation. *BMC Public Health*, 9:1–11, 2009.
- 610 [22] Ashraf S. Gorgey. Exercise awareness and barriers after spinal cord injury. *World Journal of Orthopaedics*, 5(3):158–162, 2014.
- [23] Cheri Blauwet and Stuart E. Willick. The paralympic movement: Using sports to promote health, disability rights, and social integration for athletes with disabilities. *PM and R*, 4(11):851–856, 2012.
- 615 [24] Omar W. Heyward, Riemer J.K. Vegter, Sonja De Groot, and Lucas H.V. Van Der Woude. Shoulder complaints in wheelchair athletes: A systematic review. *PLoS ONE*, 12(11):1–20, 2017.
- [25] Herre Faber, Arthur J. Van Soest, and Dinant A. Kistemaker. Inverse dynamics of mechanical multibody systems: An improved algorithm that ensures consistency between kinematics and external forces. *PLoS ONE*, 13(9):1–16, 2018.
- 625 [26] Romain Martinez, Najoua Assila, Etienne Goubault, and Mickaël Begon. Sex differences in upper limb musculoskeletal biomechanics during a lifting task. *Applied ergonomics*, 86(March):103106, 2020.
- 630 [27] Wen Wu, Peter V.S. Lee, Adam L. Bryant, Mary Galea, and David C. Ackland. Subject-specific musculoskeletal modeling in the evaluation of shoulder muscle and joint function. *Journal of Biomechanics*, 49(15):3626–3634, 2016.
- 635 [28] H. E.J. J Veeger, L. A. Rozendaal, and F. C.T. T Van Der

- Helm. Load on the shoulder in low intensity wheelchair propulsion. *Clinical Biomechanics*, 17(3):211–218, 2002.
- [29] Atsushi Inoue, Etsuo Chosa, Keisuke Goto, and Naoya Tajima. Nonlinear stress analysis of the supraspinatus tendon using three-dimensional finite element analysis. *Knee Surgery, Sports Traumatology, Arthroscopy*, 21(5):1151–1157, 2013.
- [30] Drew H. Redepenning, Paula M. Ludewig, and John M. Looft. Finite element analysis of the rotator cuff: A systematic review, jan 2020.
- [31] Yves Vanlandewijck, Daniel Theisen, and Dan Daly. Wheelchair Propulsion Biomechanics. *Sports Medicine*, 31(5):339–367, 2001.
- [32] Rory A. Cooper and Arthur Jason De Luigi. Adaptive sports technology and biomechanics: Wheelchairs. *PM and R*, 6(8 SUPPL.):31–39, 2014.
- [33] A. J. Dallmeijer, I. D.B. Zentgraaff, N. I. Zijp, and L. H.V. Van Der Woude. Submaximal physical strain and peak performance in handcycling versus handrim wheelchair propulsion. *Spinal Cord*, 42(2):91–98, 2004.
- [34] Ge Wu, Frans C.T. Van Der Helm, H. E.J. Veeger, Mohsen Makhsous, Peter Van Roy, Carolyn Anglin, Jochem Nagels, Andrew R. Karduna, Kevin McQuade, Xuguang Wang, Frederick W. Werner, and Bryan Buchholz. ISB recommendation on definitions of joint coordinate systems of various joints for the reporting of human joint motion - Part II: Shoulder, elbow, wrist and hand. *Journal of Biomechanics*, 38(5):981–992, 2005.
- [35] Michael L. Boninger, Rory A. Cooper, Rick N. Robertson, and Sean D. Shimada. Three-dimensional pushrim forces during two speeds of wheelchair propulsion. *American Journal of Physical Medicine and Rehabilitation*, 76(5), 1997.
- [36] Annet J. Dallmeijer, Luc H.V. Van der Woude, H. E.J. Veeger, and A. Peter Hollander. Effectiveness of force application in manual wheelchair propulsion in persons with spinal cord injuries. *American Journal of Physical Medicine and Rehabilitation*, 77(3), 1998.
- [37] Rick N Robertson, Michael L Boninger, Rory A Cooper, and Sean D Shimada. Pushrim Forces and Joint Kinetics During Wheelchair Propulsion. Technical report, 1996.
- [38] Jennifer L. Collinger, Michael L. Boninger, Alicia M. Koontz, Robert Price, Sue Ann Sisto, Michelle L. Tolerico, and Rory A. Cooper. Shoulder Biomechanics During the Push Phase of Wheelchair Propulsion: A Multisite Study of Persons With Paraplegia. *Archives of Physical Medicine and Rehabilitation*, 89(4):667–676, apr 2008.
- [39] S. S. Rao, E. L. Bontrager, J. K. Gronley, C. J. Newsam, and J. Perry. Three-dimensional kinematics of wheelchair propulsion. *IEEE Transactions on Rehabilitation Engineering*, 4(3):152–160, sep 1996.
- [40] Félix Chénier, Jean Philippe Pelland-Leblanc, Antoine Parrinello, Etienne Marquis, and Denis Rancourt. A high sample rate, wireless instrumented wheel for measuring 3D pushrim kinetics of a racing wheelchair. *Medical Engineering and Physics*, 87:30–37, 2021.
- [41] Weerawat Limroongreungrat, Yong Tai Wang, Li Shan Chang, Mark D. Geil, and Jeffery T. Johnson. An instrumented wheel system for measuring 3-D pushrim kinetics during racing wheelchair propulsion. *Research in Sports Medicine*, 17(3):182–194, 2009.
- [42] Michael L Boninger, Rory A Cooper, Sean D Shimada, and Thomas E Rudy. Shoulder and elbow motion during two speeds of wheelchair propulsion: a description using a local coordinate system. Technical report, 1998.
- [43] Alicia M Koontz, Rory A Cooper, Michael L Boninger, Aaron L Souza, and Brian T Fay. Shoulder kinematics and kinetics during two speeds of wheelchair propulsion. Technical Report 6, 2002.
- [44] Victoria L. Goosey, Ian G. Campbell, and Neil E. Fowler. The relationship between three-dimensional wheelchair propulsion techniques and pushing economy. *Journal of Applied Biomechanics*, 14(4):412–427, 1998.
- [45] V. L. Goosey and I. G. Campbell. Symmetry of the elbow kinematics during racing wheelchair propulsion. *Ergonomics*, 41(12):1810–1820, 1998.
- [46] A. D. Moss, N. E. Fowler, and V. L. Goosey-Tolfrey. The intra-push velocity profile of the over-ground racing wheelchair sprint start. *Journal of Biomechanics*, 38(1):15–22, 2005.
- [47] Amy R. Lewis, Elissa J. Phillips, William S. P. Robertson, Paul N. Grimshaw, and Marc Portus. Injury Prevention of Elite Wheelchair Racing Athletes Using Simulation Approaches. *Proceedings*, 2(6):255, 2018.
- [48] C Higgs. Propulsion of racing wheelchairs. *Sports and disabled athletes*, 1(2):165–172, 1984.
- [49] John W. Chow, Tim A. Millikan, Les G. Carlton, Marty I. Morse, and Woen-sik Chae. Biomechanical comparison of two racing wheelchair propulsion techniques. *Medicine and science in sports and exercise*, pages 476–484, 2001.
- [50] Y. Tai Wang, H. Deutsch, M. Morse, B. Hedrick, and T. Millikan. Three-dimensional kinematics of wheelchair propulsion across racing speeds. *Adapted Physical Activity Quarterly*, 12(1):78–89, 1995.
- [51] G. M. Gehlsen, R. W. Davis, and R. Bahamonde. Intermittent velocity and wheelchair performance characteristics. *Adapted Physical Activity Quarterly*, 7(3):219–230, 1990.
- [52] Victoria L. Goosey-Tolfrey, Neil E. Fowler, Ian G. Campbell, and Simon D. Iwnicki. A kinetic analysis of trained wheelchair racers during two speeds of propulsion. *Medical Engineering and Physics*, 23(4):259–266, 2001.
- [53] Yusuke Miyazaki, Kazuki Iida, Motomu Nakashima, Takeo Maruyama, and Kaohru Yamanobe. Measurement of push-rim forces during racing wheelchair propulsion using a novel attachable force sensor system. *Proceedings of the Institution of Mechanical Engineers, Part P: Journal of Sports Engineering and Technology*, 2020.
- [54] Philip Santos Requejo, Sara J. Mulroy, Puja Ruparel, Patricia E. Hatchett, Lisa Lighthall Haubert, Valerie J. Eberly, and Jo Anne K. Gronley. Relationship between hand contact angle and shoulder loading during manual wheelchair propulsion by individuals with paraplegia. *Topics in Spinal Cord Injury Rehabilitation*, 21(4):313–324, 2015.
- [55] Michael L. Boninger, Mark Baldwin, Rory A. Cooper, Alicia Koontz, and Leighton Chan. Manual wheelchair pushrim biomechanics and axle position. *Archives of Physical Medicine and Rehabilitation*, 81(5):608–613, 2000.
- [56] Chung Ying Tsai, Chien Ju Lin, Yueh Chu Huang, Po Chou Lin, and Fong Chin Su. The effects of rear-wheel camber on the kinematics of upper extremity during wheelchair propulsion. *BioMedical Engineering Online*, 11, nov 2012.

- [57] Yu Sheng Yang, Alicia M. Koontz, Shan Ju Yeh, and Jyh Jong Chang. Effect of backrest height on wheelchair propulsion biomechanics for level and uphill conditions. *Archives of Physical Medicine and Rehabilitation*, 93(4):654–659, apr 2012. 765
- [58] Jennifer L. Mercer, Michael Boninger, Alicia Koontz, Dianxu Ren, Trevor Dyson-Hudson, and Rory Cooper. Shoulder joint kinetics and pathology in manual wheelchair users. *Clinical Biomechanics*, 21(8):781–789, oct 2006. 770
- [59] Stefan Van Drongelen, Jos van den Berg, Ursina Arnet, Dirk Jan Veeger, and Lucas H.V. van der Woude. Development and validity of an instrumented handbike: Initial results of propulsion kinetics. *Medical Engineering and Physics*, 33(9):1167–1173, nov 2011. 775
- [60] Cassandra Kraaijenbrink, Riemer J.K. Vegter, Alexander H.R. Hensen, Heiko Wagner, and Lucas H.V. Van Der Woude. Different cadences and resistances in submaximal synchronous handcycling in able-bodied men: Effects on efficiency and force application. *PLoS ONE*, 12(8), aug 2017. 780
- [61] Lasse Jakobsen and Frederik Husted Ahlers. Development of a wireless crank moment measurement-system for a handbike: Initial results of propulsion kinetics. Technical report, 2016. 785
- [62] Barry S. Mason, Benjamin Stone, Martin B. Warner, and Victoria L. Goosey-Tolfrey. Crank length alters kinematics and kinetics, yet not the economy of recumbent handcyclists at constant handgrip speeds. *Scandinavian Journal of Medicine and Science in Sports*, 31(2):388–397, feb 2021. 790
- [63] Riemer J.K. Vegter, Barry S. Mason, Bastiaan Sporrel, Benjamin Stone, Lucas H.V. van der Woude, and Vicky L. Goosey-Tolfrey. Crank fore-aft position alters the distribution of work over the push and pull phase during synchronous recumbent handcycling of able-bodied participants. *PLoS ONE*, 14(8):1–14, 2019. 795
- [64] Oliver J. Quittmann, Joshua Meskemper, Thomas Abel, Kirsten Albracht, Tina Foitschik, Sandra Rojas-Vega, and Heiko K. Strüder. Kinematics and kinetics of handcycling propulsion at increasing workloads in able-bodied subjects. *Sports Engineering*, 21(4):283–294, 2018. 800
- [65] Oliver J. Quittmann, Thomas Abel, Kirsten Albracht, and Heiko K. Strüder. Biomechanics of all-out handcycling exercise: kinetics, kinematics and muscular activity of a 15-s sprint test in able-bodied participants. *Sports Biomechanics*, 2020. 805
- [66] Frederik Husted Ahlers and Lasse Jakobsen. Biomechanical analysis of hand cycling propulsion movement : A musculoskeletal modelling approach. Technical report, 2016. 810
- [67] Arnaud Faupin, Philippe Gorce, Eric Watelain, Christophe Meyer, and Andre Thevenon. A biomechanical analysis of handcycling: A case study. *Journal of Applied Biomechanics*, 26(2):240–245, 2010. 815
- [68] Benjamin Stone, Barry S. Mason, Martin B. Warner, and Victoria L. Goosey-Tolfrey. Shoulder and thorax kinematics contribute to increased power output of competitive handcyclists. *Scandinavian Journal of Medicine and Science in Sports*, 29(6):843–853, 2019. 820
- [69] Emanuele Chiodi. *A biomechanical model of the upper limb applied to the handcycling*. PhD thesis, 2016.
- [70] Arnaud Faupin and Philippe Gorce. The effects of crank adjustments on handbike propulsion: A kinematic model approach. *International Journal of Industrial Ergonomics*, 38(7-8):577–583, jul 2008. 825
- [71] M. B. Warner, P. H. Chappell, and M. J. Stokes. Measuring scapular kinematics during arm lowering using the acromion marker cluster. *Human Movement Science*, 31(2):386–396, 2012. 830
- [72] D. J.J. Bregman, S. van Drongelen, and H. E.J. Veeger. Is effective force application in handrim wheelchair propulsion also efficient? *Clinical Biomechanics*, 24(1):13–19, jan 2009.
- [73] Ann M. Cools, Fredrik R. Johansson, Dorien Borms, and Annelies Maenhout. Prevention of shoulder injuries in overhead athletes: A science-based approach. *Brazilian Journal of Physical Therapy*, 19(5):331–339, 2015. 835
- [74] Ursina Arnet. *Handcycling : a biophysical analysis*. 2012.
- [75] Deborah A. Nawoczenski, Linda M. Riek, Lindsey Greco, Katharine Staiti, and Paula M. Ludewig. Effect of shoulder pain on shoulder kinematics during weight-bearing tasks in persons with spinal cord injury. *Archives of Physical Medicine and Rehabilitation*, 93(8):1421–1430, 2012. 840

Figures created with BioRender.com

845

Supplemental Data

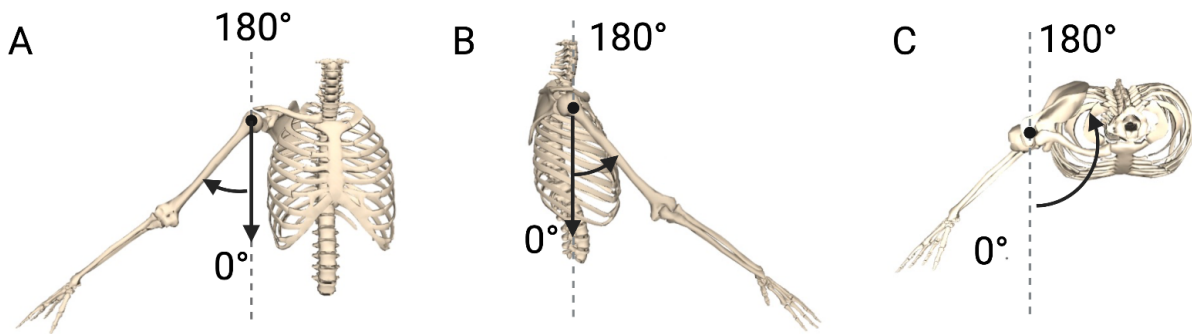


Figure S1: Joint angle conventions based on ISB standards for A) shoulder abduction / adduction, B) shoulder flexion / extension in the sagittal plane, and C) shoulder internal / external rotation. Angles are defined as the angle of the humerus relative to the thorax.